Transport in Porous Media **2** (1987) 301–316

Effective and Relative Permeabilities of Anisotropic Porous Media

JACOB BEAR, CAROL BRAESTER, and PASCAL C. MENIER
Technion – Israel Institute of Technology, Haifa 32000, Israel

(Received: 27 August 1986; revised: 26 January 1987)

Abstract. A model composed of a three-dimensional orthogonal network of capillary tubes was used to simulate the flow behavior in an unsaturated anisotropic soil. The anisotropy in the network's permeability was introduced by randomly selecting the radii in the three mutually orthogonal directions of the network tubes from three different lognormal probability distributions, one for each direction. These three directions were assumed to be the principal directions of anisotropy. The sample was gradually drained, with only tubes smaller than a certain diameter remaining full at each degree of saturation. Computer experiments were conducted to determine the network's effective permeability as a function of saturation. The main conclusion was that the relationship between saturation and effective permeability depends on direction. Consequently the concept of relative permeability used in unsaturated flow should be limited to isotropic media and not extended to anisotropic ones.

Key words. Effective permeability, relative permeability, anisotropy, unsaturated flow, capillary tube network.

1. List of Symbols

f_r relative frequency of pores in the network,
$f(r)$ probability density function of tube radii,
$F(r)$ cumulative probability density function of radii,
g gravity acceleration,
k permeability,
k_{ij} permeability tensor components,
k_{wa} directional permeability to water in the direction of flow,
l length of capillary tube,
L length of network of capillary tubes,
m mean,
p pressure,
p_c capillary pressure,
q specific flux,
Q rate of flow,
r radius,
$r_{\min}$ minimum radius,
$r_{\max}$ maximum radius,
S saturation,

S_{ir} irreducible saturation,
S_r residual saturation,
S_e effective saturation,
v variance,
x, y, z Cartesian coordinates,
x_j Cartesian coordinate in the j direction, $j = 1, 2$ and 3 corresponding to x, y, and z directions, respectively,

Greek

ρ fluid density,
μ dynamic viscosity,
σ surface tension,

Subscripts

a air,
r relative,
w water.

2. Introduction

Phenomena of multiphase flow in porous media occur in many fields of practical engineering interest. Some examples are the flow of air and water in soils, the flow of oil, gas and water in petroleum reservoirs, and the flow of steam and water in geothermal reservoirs. In the present paper, we focus our attention mainly on the example of air-water (=unsaturated) flow in soils. However, the conclusions derived for this particular case may be extended to the general case of multiphase flow. Most of the work conducted hitherto on multiphase flow has been related to isotropic porous media. This observation is valid for both theoretical studies as well as for laboratory and field investigations. In the latter cases, isotropy is usually *assumed*. In the work reported here, we consider anisotropic flow domains in which the anisotropy is due to the nature of the microscopic configuration of the void space.

As is well known, because of the lack of detailed information concerning the configuration of the void space, we cannot model flow and phenomena of transport through porous media at the *microscopic* level. Instead, the actual domain, occupied partly by a solid phase and partly by one or more fluid phases, may be replaced by a continuum. At every point of this continuum, and at every instant of time, kinematic and thermodynamic variables can be assigned for each phase present in the system. In this way, variables at the continuum level are continuous differentiable functions of the spatial coordinates and of time.

The passage from the microscopic level of description to the *macroscopic* one is carried out by averaging the former over the *representative elementary volume*

(REV) of the porous medium domain (e.g., Hassanizadeh and Gray, 1979; Bear and Bachmat, 1984).

In the present investigation, we consider a model of a porous medium that has the size of an REV, and two fluid phases, air and water, that together occupy its entire void space. The void space configuration causes the permeability to each of the two phases to be anisotropic. This model will be used for investigating the effect of saturation on the anisotropy in permeability.

The motion equation (Darcy's law) for a single fluid that saturates the entire void space can be written in the form

$$q_i = -\frac{k_{ij}}{\mu}\left(\frac{\partial p}{\partial x_j} + \rho g \frac{\partial z}{\partial x_j}\right) \quad (i, j = 1, 2, 3) \tag{1}$$

where q_i is the ith component of the specific discharge vector, p is pressure, μ is dynamic viscosity, z is the vertical coordinate (positive upwards), ρ is fluid density, g is gravity acceleration, and k_{ij} are the components of the permeability (or effective permeability) – a second rank symmetric tensor. For an isotropic porous medium, the permeability reduces to a scalar, k. For the sake of simplicity we shall assume here that the solid matrix is stationary and nondeformable.

In unsaturated flow, with movement of both air and water, Darcy's law is written separately for each phase (e.g., Bear, 1972)

$$\begin{aligned} q_{ai} &= -\frac{k_{aij}}{\mu_a}\left(\frac{\partial p_a}{\partial x_j} + \rho_a g \frac{\partial z}{\partial x_j}\right) \quad (i, j = 1, 2, 3), \\ q_{wi} &= -\frac{k_{wij}}{\mu_w}\left(\frac{\partial p_w}{\partial x_j} + \rho_w g \frac{\partial z}{\partial x_j}\right) \quad (i, j = 1, 2, 3), \end{aligned} \tag{2}$$

where subscripts a and w denote air and water, respectively, and $k_{aij}(S_w)$ and $k_{wij}(S_w)$ are the effective permeabilities to air and water, respectively. Since each phase occupies only part of the void space, these effective permeabilities must be functions of the respective saturations. In an anisotropic porous medium, the two effective permeabilities reduce to scalar functions $k_a(S_w)$ and $k_w(S_w)$.

The pressure in the air (nonwetting phase) and in the water (wetting phase) are related to each other through the capillary pressure, p_c, which is a function of saturation

$$p_c(S_w) = p_a - p_w . \tag{3}$$

In writing (2) we have indicated that in an anisotropic porous medium, the effective permeabilities $k_a(S_w)$ and $k_w(S_w)$ are also second rank (symmetric) tensors. This can be rigorously shown by averaging the Navier–Stokes equations for a fluid that occupies only part of the void space (e.g., Bear and Bachmat, 1987).

A normalized effective permeability – called *relative permeability* k_r – is often used in two-phase flow in isotropic porous media. It is defined as the ratio of effective permeability to the corresponding permeability at saturation.

$$k_{ar}(S_w) = k_a(S_w)/k, \qquad k_{wr}(S_w) = k_w(S_w)/k. \tag{4}$$

Various expressions, based on experimental results, are suggested in the literature for the relationship between the relative permeability and the *effective saturation*, defined by $S_e = (S_w - S_{wir})/(1 - S_{wir})$ where S_{wir} is the *irreducible water saturation*, i.e., the saturation at which the effective permeability to water reduces to zero, due to the fact that the water phase is no more a continuous phase within the void space. A typical example for the dependence of relative permeability on saturation is (Corey, 1954)

$$k_{wr}(S_w) = S_e^4. \tag{5}$$

Although not generally valid (Bruckstern and Morel-Seytoux, 1970), in many practical cases it is assumed that the mobility of the air is relatively large so that the air pressure is uniform and equal to the atmospheric pressure (usually taken as a reference pressure, equal to zero). Here we shall also make this assumption. It should not affect the main conclusions of this study.

Many authors extend the concept of relative permeability, as defined above, to anisotropic porous media, by *assuming that $k_{wr}(S_w)$ is independent of direction*. For example, Collins (1961) suggests that along the x, y, and z directions, relative permeabilities be defined as

$$k_{wr}(S_w) = k_{wx}(S_w)/k_x = k_{wy}(S_w)/k_y = k_{wz}(S_w)/k_z \tag{6}$$

where k_x, k_y and k_z are the principal values of the permeability tensor at saturation. Other authors (e.g., Mustafa and Marslia, 1983, and authors cited by them) extend the same assumption to the general case of x, y and z which are not principal directions and write

$$k_{wr}(S_w) = k_{wij}(S_w)/k_{ij} \tag{7}$$

i.e., *the functional dependence* of k_{wr} on S_w *is the same for all directions*.

As stated above, the purpose of this study is to investigate the relationship between relative permeability and direction in an anisotropic porous medium in order to examine the validity of (7).

The investigation reported here is based on *computer experiments* conducted on a model composed of a three-dimensional orthogonal network of capillary tubes, believed to simulate the behavior of a representative sample of an anisotropic real soil in unsaturated air-water flow. Our basic requirements are that the model's size represent an REV, and that its behavior, as manifested by the relationships between the effective permeability and saturation and between capillary pressure and saturation, be similar to those exhibited by a real porous medium.

3. The Capillary Tube Network Model

Fatt (1956) introduced the two-dimensional capillary tube network as a model of a porous medium and demonstrated its capability to simulate the characteristic

behavior of porous media. Fatt's study was limited to isotropic media. Since then, the capillary tube network has been extensively used for various purposes (Dullien, 1975; Partom, 1978). Reviews on the use of network models were published by Chatazis and Dullien (1978) and Dullien (1979).

In analogy to the variation in pore size of a real porous medium, the network is composed of tubes of different radii. In analogy to the fluid distribution in an actual porous medium, in which certain pores are occupied by the wetting fluid while others are occupied by the nonwetting one, we require that part of the total number of tubes be occupied by the wetting fluid, while the remaining tubes be filled by the nonwetting one.

The resistance to flow manifested by the pores is simulated by the resistance of the capillary tubes, obtained from Poiseuille law for flow in the latter. The network of the capillary tubes should be such that its permeability-saturation relationship be the same as that of the real porous medium.

Finally, because the network, as a whole, represents an REV of a real porous medium, the considered network should consist of a sufficiently large number of tubes.

Some characteristic properties of capillary tube network models are (Fatt, 1956; Shante and Kirkpatrick, 1971; Dullien, 1979) the *dimensionality* of the network, e.g., two- or three-dimensional, the *connection factor*, Y, and the *coordination number*, Z, defined by

$$Y = \Sigma_{(r)}\, Y_r f_r, \quad \text{with } Y_r = (\Sigma p)_r \tag{8}$$

and

$$Z = \Sigma_{(r)}\, Z_r f_r, \quad \text{with } Z_r = 0.5\ Y_r + 1 \tag{9}$$

where $(\Sigma p)_r$ is the number of pores (=segments of capillary tubes) connected to a pore of type r at both ends and f_r is the relative frequency of such pores in the network.

The network chosen in the present study consists of a regular three-dimensional network of mutually orthogonal straight capillary tubes. This is the simplest and the least computer time consuming model that enables the simulation of an anisotropic porous medium. Anisotropy is obtained by assigning different average resistances to each of the three network directions.

In each direction, the radii of the tubes are considered a random variable. Lognormal probability distributions were found suitable for describing pore (or grain) size distributions. Consequently, such a distribution was chosen as the probability density function for the capillary tube radii in the model.

To allow for a lower and an upper bound of the tube radii, a modified lognormal distribution (Johnson, 1949a, 1949b; Aitchison and Brown, 1957), was used. This lognormal distribution is characterized by the following four parameters: the minimum radius ($r_{\min}$), the maximum radius ($r_{\max}$), the mean (m)

and the variance (v). The cumulative distribution function is given by

$$F(r) = \int_{r_{\min}}^{r} f(r)\,\mathrm{d}r = [(r_{\max} - r_{\min})/(2\pi v)^{1/2}] \times$$
$$\times \int_{r_{\min}}^{r} \frac{1}{(r_{\max} - r)(r - r_{\min})} \exp\left(\frac{\left[\ln\left(\frac{r - r_{\min}}{r_{\max} - r}\right) - m\right]^2}{2v}\right)\mathrm{d}r \tag{10}$$

where $f(r)$ is the probability density function and v is the variance.

The calculation of an effective permeability value for the network of capillaries requires the following steps.

First, the Monte Carlo technique is employed for assigning values to the network's tube radii, in accordance with the distribution function given by (10). A realization of an anisotropic network is generated by using a different distribution function for the radii of the tubes oriented in each of the three orthogonal directions. Once tube radii have been assigned, the (equal) length of the tubes is calculated so as to match the porosity of the porous medium sample simulated by the network.

In the second step, we prescribe a capillary pressure, p_c, and determine the wetting fluid distribution that corresponds to that pressure. The relationship between the capillary pressure and the radius of a tube

$$r = 2\sigma/p_c \tag{11}$$

where σ is the surface tension and where the contact angle was assumed to be equal to zero, is used to determine which tubes will be occupied by the wetting fluid. This equation states that air can enter a tube if the radius of that tube is larger than that which corresponds to the considered capillary pressure.

With the above relationship between the capillary pressure and radius, the sample is desaturated by starting from a low capillary pressure value and proceeding to drain the sample by increasing the capillary pressure in steps until the wetting phase becomes discontinuous. At this point, further drainage is not possible.

To obtain the effect of anisotropy, desaturation and flow experiments on each realization were performed separately for each of the three directions, parallel to the tube orientations. During each experiment, flow was allowed only through the boundary planes that were perpendicular to the flow direction, while the other boundaries were made impervious. Accordingly, during desaturation the wetting fluid was allowed to enter, and the wetting fluid to leave the network only through the inlet and outlet boundaries. Desaturation also required that a continuous path of wetting fluid exist from the considered tube to the outlet. To determine the fluid distribution for every value of capillary pressure, the network was scanned systematically from the inlet to the outlet boundary and the tubes were declared full or desaturated, according to the principle explained above.

The network was scanned several times until no additional tubes could be desaturated. At the end of each run, the saturation corresponding to the considered capillary pressure value was recorded, thus obtaining a point on the *retention curve* $p_c = p_c(S_w)$.

Finally, the effective permeability was calculated for every network realization, for every capillary pressure and for each of the three orthogonal directions. For each direction, the pressure boundary conditions imposed on opposite boundaries were such that an average flow in that direction was simulated. The permeability in the considered direction was determined from the results of a flow experiment under steady state conditions, with an imposed pressure difference between the inlet and outlet boundaries.

The flow rates through the network's tubes that remained full with the wetting fluid, was determined from the volumetric balance equations written for every node, requiring that the algebraic sum of the fluxes at a node equals zero. For a node with coordinates $x = il$, $y = jl$ and $z = kl$, where l is the length of the tube (Figure 1) the volumetric balance equation is

$$Q_{i-1,j,k} + Q_{i+1,j,k} + Q_{i,j-1,k} + Q_{i,j+1,k} + Q_{i,j,k-1} + Q_{i,j,k+1} = 0. \tag{12}$$

The Hagen–Poiseuille law was invoked for the calculation of the rate of flow through a capillary tube

$$Q = \frac{\pi r^4}{8\mu} \frac{\Delta p}{1} \tag{13}$$

where Δp is the pressure difference between the end points of the tube.

Substituting (13) into (12), we obtain

$$\begin{aligned} &C_{i-1,j,k}(p_{i-1,j,k} - p_{i,j,k}) + C_{i-1,j,k}(p_{i,j,k} - p_{i+1,j,k}) + \\ &+ C_{i,j-1,k}(p_{i,j-1,k} - p_{i,j,k}) + C_{i,j+1,k}(p_{i,j,k} - p_{i,j+1,k}) + \\ &+ C_{i,j,k-1}(p_{i,j,k-1} - p_{i,j,k}) + C_{i,j,k+1}(p_{i,j,k} - p_{i,j,k+1}) = 0 \end{aligned} \tag{14}$$

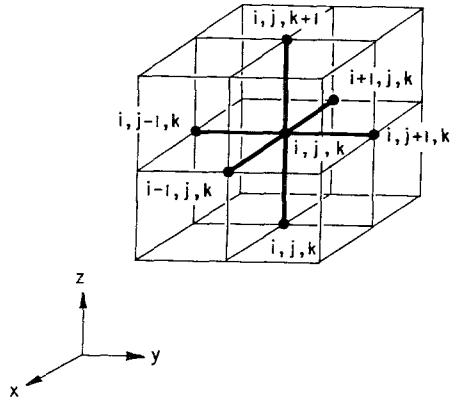

Fig. 1. Sketch for capillary tube network and node designation.

where

$$C_{i-1,j,k} = (\pi/8\mu l) r^4_{i-1,j,k}. \tag{15}$$

Relationships similar to (15) also hold for all other tubes. By writing (15) for every node, a system of algebraic equations was obtained and solved under the imposed boundary conditions. The solution gave the pressure at every network node. The rate of flow through the inlet and outlet boundaries was calculated from the fluxes through the individual boundary tubes. The equivalent effective permeability was determined by writing Darcy's law for the average flow, i.e.,

$$k = \frac{Q}{L}\frac{\mu}{\Delta p} \tag{16}$$

where L is the length of the sample (cube), and Δp is the imposed pressure difference between the inlet and outlet boundaries.

The entire effective permeability curve was obtained by repeating the above calculation for each saturation step. The drainage process terminated when the tubes that remain full do not form a continuous subnetwork that permitted flow from one boundary to the other. At this point (irreducible saturation), the permeability vanished. Thus, the irreducible saturation was also determined for every network realization.

The complete effective permeability curve was determined for every network realization. The behavior of the actual sample was assumed to be represented by the average of the different realizations.

4. Computer Runs and Results

Because of the randomness of the spatial distribution of the tube radii, a sufficiently large number of tubes is required in order to obtain a sample that has the size of an REV and thus yield results that are independent of the network size. Also, the entire procedure has to be repeated for a sufficiently large number of realizations, in order to eliminate the effect of the random selection of the radii.

There is an interchange between the size (i.e., number of tubes) and the number of realizations required to obtain results for retention curves and effective permeability curves that are independent of sample size and of the random selection of radii.

Accordingly, the number of realizations and the size of the network were determined simultaneously such that the oscillation of the average values of calculated parameters were reduced to within an acceptable range. The size of the REV, i.e., the total number of tubes, may differ for different properties.

In the present case, we considered a network of $11 \times 11 \times 11$ nodes (and 3636 tubes) and checked the oscillations in the averaged effective permeability, which is the relevant parameter in the present problem. Figure 2 presents the results of

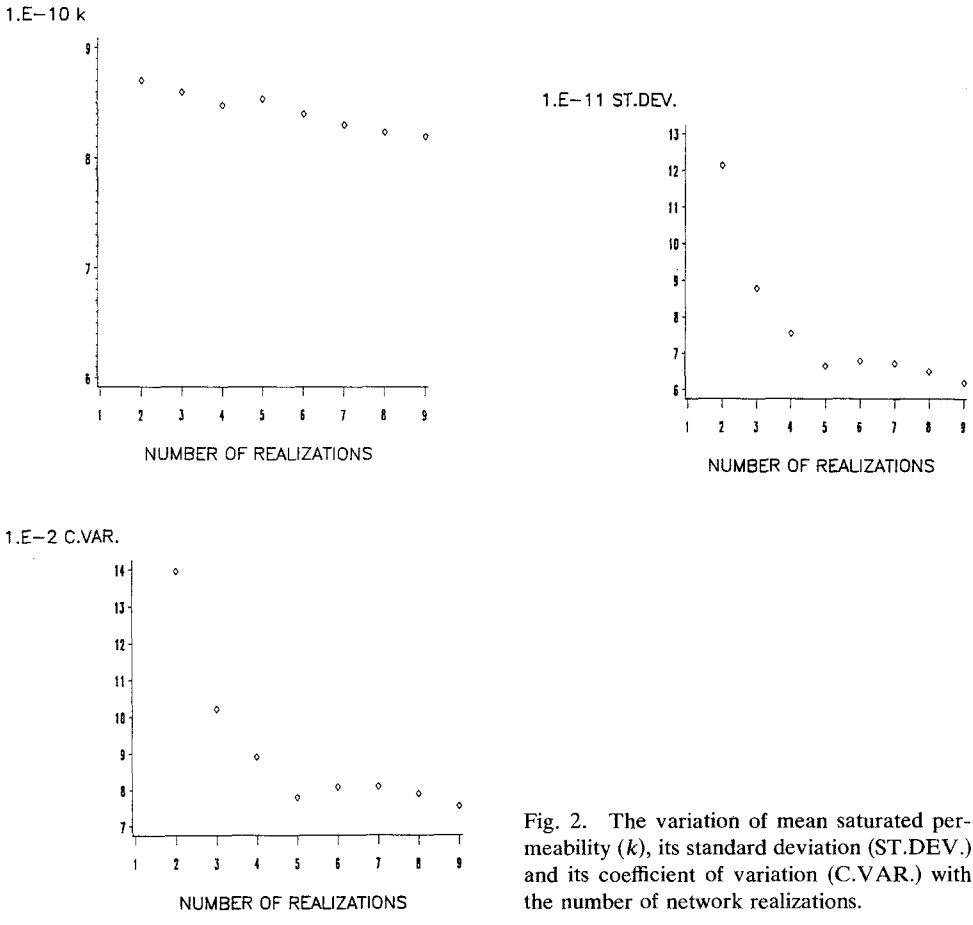

Fig. 2. The variation of mean saturated permeability (k), its standard deviation (ST.DEV.) and its coefficient of variation (C.VAR.) with the number of network realizations.

numerical experiments in the form of mean, of the standard deviation and the coefficient of variation of permeability in the x direction at full saturation as a function of the number of realizations. The lognormal radii distribution for the x direction of the run series 2A (see below) was used. A similar behavior was also found for all other radii probability distribution functions and other saturations. Hence, 12 realizations were selected as satisfactory for the network of $11 \times 11 \times 11$ nodes considered here.

The objective of the first series of runs (runs 11) was to demonstrate the capability of the capillary tube network model to simulate the capillary pressure and the effective permeability of an isotropic porous medium and their dependence on saturation. The considered porous medium was made of glass beads (Brooks and Corey, 1964). The matching of the model was obtained by adjusting the parameters of the lognormal distribution of tube radii. The irreducible water saturation was matched by randomly eliminating from the beginning a certain number of tubes from the network. A fairly good fit of the capillary pressure and

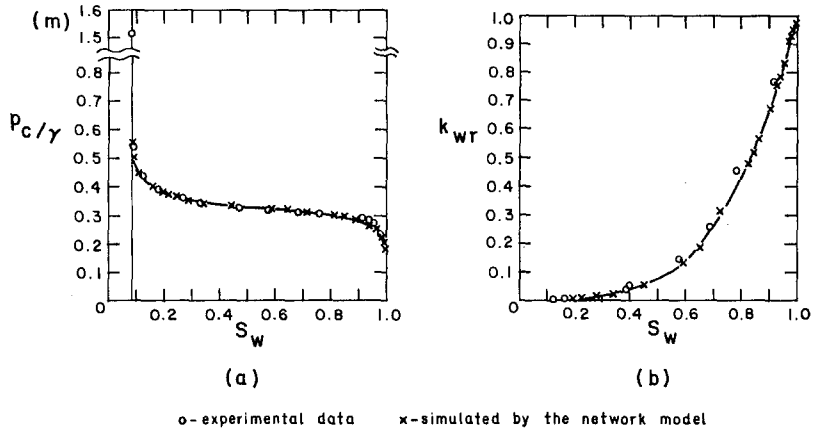

Fig. 3. Comparison of laboratory experiments (Brooks and Corey, 1964) and computer simulated capillary pressure (a) and relative permeability (b) curves. Porosity = 0.37 and the irreducible water saturation = 0.085.

of the relative permeability curves (Figure 3) was obtained with the following set of the parameters of the lognormal distribution: $r_{min} = 10 \times 10^{-6}$ m, $r_{max} = 150 \times 10^{-6}$ m, $m = 3.835$ and $v = 0.046$.

On the basis of these experiments we reached the conclusion that the capillary tube network is capable of simulating also the characteristic features of anisotropic porous media, e.g., the anisotropic effective permeability.

Two additional series of runs were performed with anisotropic networks (Series 1A and 2A).

In the runs of Series 1A, the same probability functions were used for the x and y directions, while in the z direction the probability function was different. We have thus simulated anisotropy with axial symmetry. The purpose of these runs was to demonstrate that the desaturation of an isotropic sample (in the present case, isotropy of the x and y directions) does not introduce any anisotropy. The considered lognormal distribution parameter values for the x and the y directions were $r_{min} = 3 \times 10^{-5}$ m, $r_{max} = 6 \times 10^{-5}$ m, $m = -1.1$ and $v = 0.75$. For the z direction the parameter values were $r_{min} = 3 \times 10^{-5}$ m, $r_{max} = 6 \times 10^{-5}$ m, $m = -1.1$ and $v = 10.0$. The results for relative permeabilities and for anisotropy permeability ratios as functions of saturation, are presented in Figure 4 and Table I.

In the runs of Series 2A different probability functions were used for the x, y and z directions. The four parameters of the radii lognormal probability distribution were: in the x direction $r_{min} = 1 \times 10^{-5}$ m, $r_{max} = 100 \times 10^{-5}$ m, $m = -1$ and $v = 0.75$; in the y direction $r_{min} = 1 \times 10^{-5}$ m, $r_{max} = 100 \times 10^{-5}$ m, $m = -2$ and $v = 0.75$ and in the z direction $r_{min} = 1 \times 10^{-5}$ m, $r_{max} = 100 \times 10^{-5}$ m, $m = -3$ and $v = 0.75$. The results of the runs Series 2A are presented in Figure 5 and Table II.

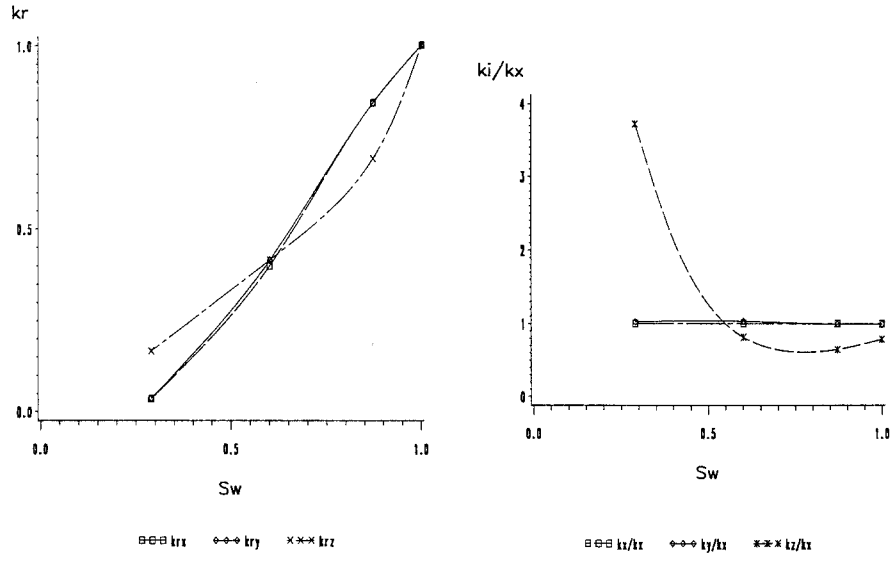

Fig. 4. Results of run Series 1A: (a) relative permeability and (b) anisotropy ratios.

The results show that for an anisotropic sample, the relative permeability, defined for each direction as the ratio of the effective permeability to the respective permeability at saturation, is not a unique function but is strongly direction dependent.

In runs of both Series 1A and 2A, the permeability in the z direction (and in case 2A also in the y direction) at full saturation is smaller than in the x

Table I. Results of runs of Series 1A

Dir.	Sat.	k_{mean}	k_r	Standard deviation	Coef. of variation	k_i/k_x
x	1.000	0.1868E − 10	1.000	0.2600E − 12	0.1392E − 01	
y	1.000	0.1860E − 10	1.000	0.2288E − 12	0.1230E − 01	0.996
z	1.000	0.1468E − 10	1.000	0.4279E − 12	0.2915E − 01	0.786
x	0.871	0.1576E − 10	0.844	0.4250E − 12	0.2697E − 01	
y	0.871	0.1569E − 10	0.843	0.3790E − 12	0.2416E − 01	0.995
z	0.871	0.1017E − 10	0.692	0.2970E − 12	0.2922E − 01	0.645
x	0.601	0.7477E − 11	0.400	0.2342E − 12	0.3132E − 01	
y	0.601	0.7722E − 11	0.415	0.3646E − 12	0.4721E − 01	1.033
z	0.601	0.6089E − 11	0.415	0.2418E − 12	0.3970E − 01	0.814
x	0.289	0.6529E − 12	0.035	0.1049E − 12	0.1607E + 00	
y	0.289	0.6683E − 12	0.036	0.8441E − 13	0.1263E + 00	1.024
z	0.289	0.2433E − 11	0.166	0.2412E − 12	0.9914E − 01	3.727

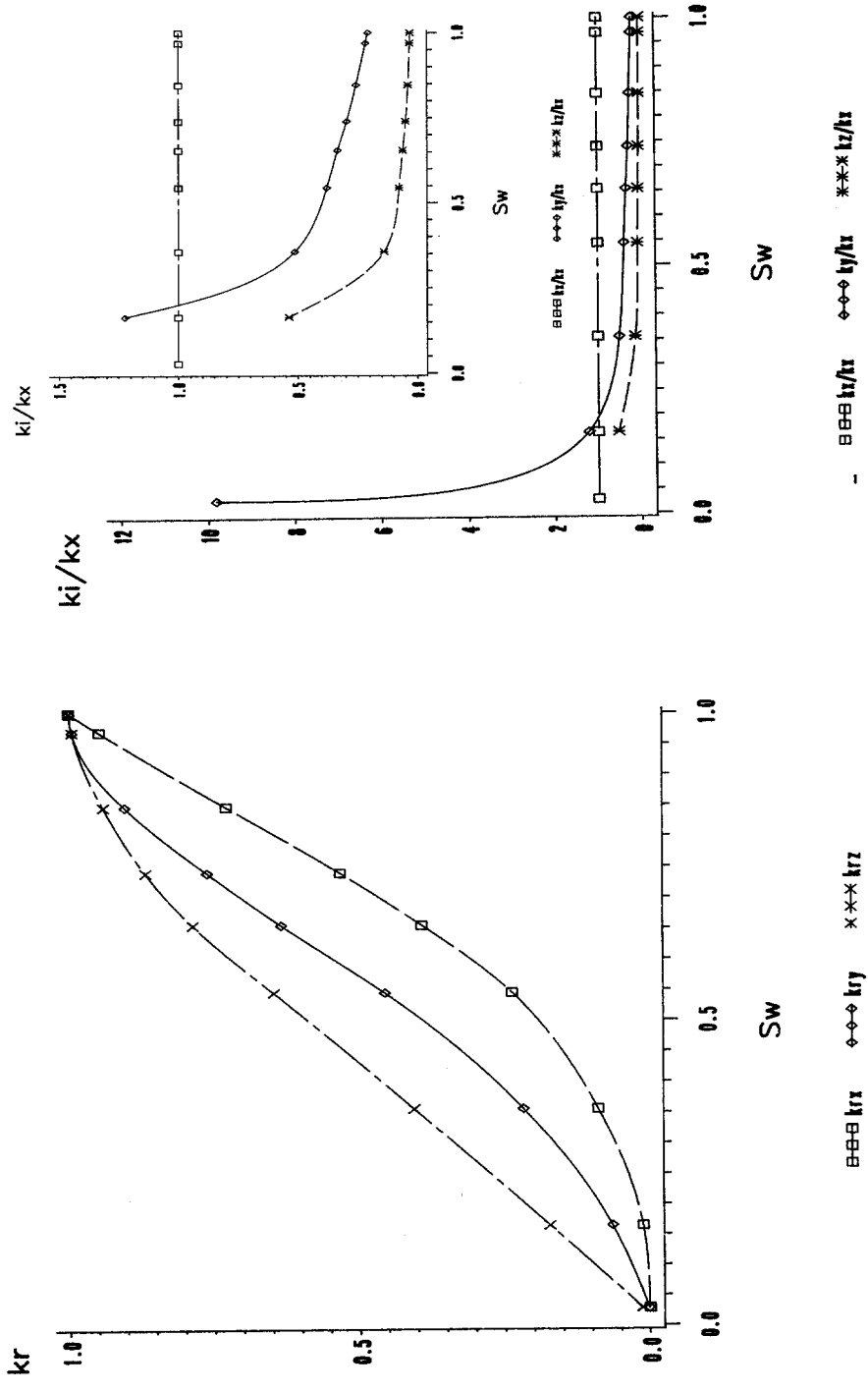

Fig. 5. Results of run Series 2A: (a) relative permeability and (b) anisotropy ratios.

Table II. Results of runs of Series 2A

Dir.	Sat.	k_{mean}	k_r	Standard deviation	Coef. of variation	k_i/k_x
x	1.000	0.8197E−09	1.000	0.6192E−10	0.7554E−01	
y	1.000	0.1697E−09	1.000	0.1183E−10	0.6970E−01	0.207
z	1.000	0.2483E−10	1.000	0.3449E−11	0.1389E+00	0.030
x	0.969	0.7763E−09	0.947	0.6890E−10	0.8875E−01	
y	0.969	0.1686E−09	0.994	0.1164E−10	0.6904E−01	0.217
z	0.969	0.2469E−10	0.994	0.3439E−11	0.1393E+00	0.032
x	0.846	0.5965E−09	0.728	0.7050E−10	0.1182E+00	
y	0.846	0.1532E−09	0.903	0.1013E−10	0.6611E−01	0.257
z	0.846	0.2335E−10	0.940	0.3420E−11	0.1465E+00	0.039
x	0.739	0.4364E−09	0.532	0.3051E−10	0.6991E−01	
y	0.739	0.1291E−09	0.761	0.7220E−11	0.5592E−01	0.296
z	0.739	0.2129E−10	0.867	0.3010E−11	0.1414E+00	0.049
x	0.654	0.3205E−09	0.391	0.3310E−10	0.1033E+00	
y	0.654	0.1102E−09	0.634	0.5540E−11	0.5027E−01	0.344
z	0.654	0.1951E−10	0.786	0.2806E−11	0.1439E+00	0.061
x	0.544	0.1933E−09	0.236	0.1963E−10	0.1015E+00	
y	0.544	0.7720E−10	0.455	0.6719E−11	0.8703E−01	0.399
z	0.544	0.1606E−10	0.647	0.2140E−11	0.1332E+00	0.083
x	0.355	0.7190E−10	0.088	0.1159E−10	0.1611E+00	
y	0.355	0.3688E−10	0.217	0.4992E−11	0.1353E+00	0.513
z	0.355	0.1007E−10	0.405	0.9626E−12	0.9562E−01	0.140
x	0.164	0.8872E−11	0.011	0.2795E−11	0.3151E+00	
y	0.164	0.1085E−10	0.064	0.1649E−11	0.1520E+00	1.223
z	0.164	0.4764E−11	0.172	0.5269E−12	0.1106E+00	0.537
x	0.028	0.1077E−13	0.000	0.3716E−14	0.3450E+00	
y	0.028	0.1057E−12	0.001	0.3505E−13	0.3314E+00	9.819
z	0.028	0.3207E−12	0.013	0.4917E−13	0.1533E+00	29.774

direction. As saturation decreases, at a certain saturation the value of the permeability in the z direction equals that in the x direction; for still lower desaturations, the anisotropy is reversed, i.e., the permeability in the z direction becomes larger than in the x direction. In Series 2A with different permeabilities in the y and x directions, the permeability in the y direction exhibits a similar behavior. For instance, in Series 2A, the anisotropy ratios at full saturation are $k_y/k_x = 0.207$ and $k_z/k_x = 0.030$. At a saturation of approximately 0.2, the medium becomes isotropic in the x and y directions, while in the z direction the anisotropy ratio is $k_z/k_x = 0.55$. At a lower saturation, the medium becomes isotropic in the z direction, while in the y direction the anisotropy is reversed in comparison to that at full saturation. At lower saturations the anisotropy in the z direction is also reversed in comparison to that at full saturation.

5. The Tensorial Nature of Effective and Relative Permeabilities

It is important to recall at this point that it has been implicitly assumed by many researchers that the principal axes of the effective permeability do not rotate when the saturation varies.

To the best of our knowledge, the assumption of fixed principal directions has never been formally proven. However, it seems that at least for the cubic network investigated here, this assumption is not worse than to assume that the principal directions of the network are in the direction of the capillary tubes at saturation $S_w = 1$.

For any given value of saturation, or effective saturation, a knowledge of the corresponding values of the principal effective permeabilities, enables us to determine the off-diagonal components of the effective permeability tensor. The reader is referred to the literature (e.g., Bear, 1972) for the formulas and Mohr's circle method for performing this transformation.

Another possible representation of the effective permeability tensor is to plot on a polar diagram (Figure 6) the locus of the square root of the directional effective permeability, in the direction of the specific flux q. For each value of the

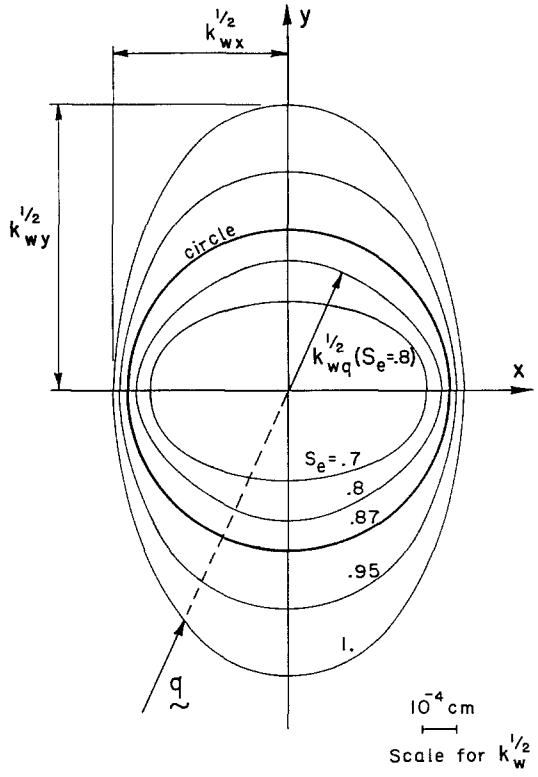

Fig. 6. Ellipses of directional permeability, $k_{wq}(S_e)$.

effective saturation we have a separate ellipse. We could also draw ellipses for the directional effective permeability in the direction of the gradient (see discussion in Bear, 1972, p. 144).

We come now to the relative permeability. There is no difficulty in using this concept in the case of an anisotropic porous medium, as long as we stay with principal directions. We write, for example

$$\begin{vmatrix} k_{rx}(S_e) & 0 \\ 0 & k_{ry}(S_e) \end{vmatrix} \begin{vmatrix} k_x & 0 \\ 0 & k_y \end{vmatrix} = \begin{vmatrix} k_{wx}(S_e) & 0 \\ 0 & k_{wy}(S_e) \end{vmatrix}, \tag{17}$$

i.e., with

$$k_{rx}(S_e)k_x = k_{wx}(S_e); \qquad k_{ry}(S_e)k_y = k_{wy}(S_e). \tag{18}$$

However, *we cannot extend the concept and definition of relative permeability to the general case of anisotropy when x, y and z are not principal directions.* We cannot use the definition

$$k_{rij} = k_{wij}/k_{ij} \quad \text{(no summation on } i, j \text{ is implied)} \tag{19}$$

for relative permeability and then regard the relative permeability as a second rank tensor such that

$$k_{rim}(S_e)k_{mj} = k_{wij}(S_e) \quad \text{(summation convention implied)} \tag{20}$$

unless $k_{wij} = 0$ and $k_{ij} = 0$ for $i = j$.

Accordingly, our conclusion is that the components of relative permeability as defined by (19) are not components of a second rank tensor.

In principle, it is possible to *define* a relative permeability tensor with components defined by (20). However, we do not see any advantage in doing so. Hence, we propose that the concept of relative permeability be restricted to isotropic porous media only.

6. Conclusions

The main feature investigated here was the influence of changes in saturation on the effective permeability in flow through anisotropic porous media. The study was carried out by conducting computer experiments on a three-dimensional network composed of three mutually orthonal sets of capillary tubes, with randomly selected radii.

The main conclusions of the present study are:

(a) In an anisotropic porous medium, the effect of saturation on the effective permeability depends on direction, and

(b) The concept of relative permeability, as defined and often used in dealing with unsaturated flow in isotropic media, should not be extended to flow in anisotropic porous media. With the common definition (=ratio of components of effective permeability to corresponding components of saturated permeability),

the components of relative permeability do not constitute components of a second rank tensor. Thus, there seems to be no advantage in extending the definition and concept of relative permeability to anisotropic porous media.

The main drawback of the model employed here is that the capillary tubes were oriented only in three directions, and not oriented randomly in space.

Acknowledgement

The work was partly supported by the fund for the promotion of research at the Technion. Part of this research originated from a Msc thesis of Menier Pascal prepared under the supervision of Prof. Jacob Bear.

References

Aitchison, J. and Brown, J. A. C., 1957, *The Lognormal Distribution*, University Press, Cambridge.

Bear, J., 1972, *Dynamics of Fluids in Porous Media*, Elsevier, N.Y.

Bear, J. and Bachmat, Y., 1984, Transport phenomena in porous media – Basic equations, in J. Bear and Y. Corapicoglu (eds.) *Fundamentals of Transport Phenomena in Porous Media*, Martinus Nijhoff, Dordrecht, pp. 3–61.

Bear, J. and Bachmat, Y., 1987, *Introduction to Modeling of Transport Phenomena in Porous Media*, D. Reidel, Dordrecht, (under preparation).

Brooks, R. H. and Corey, A. T., 1964, Hydraulic properties of porous media, Hydrology paper No. 3, Colorado State University, Fort Collins, Colo.

Bruckstern, R. L. and Morel-Seytoux, H. J., 1970, Analytical treatment of two-phase infiltration, *J. Hy. Div. of Proc. ASCE*, 2535–2548.

Chatazis, I. and Dullien, F. A. L., 1978, A network approach to analyze and model capillary and transport phenomena in porous media, *IAHR Symposium, Thessaloniki, Greece*, 1.1–1.22.

Collins, R. E., 1961, *Flow of Fluids through Porous Materials*, Reinhold, N.Y.

Corey, A. T., 1954, The interrelation between gas and oil relative permeabilities, *Prod. Monthly* **19**, 38–41.

Dullien, F. A. L., 1975, New network permeability model of porous media, *AICRE* **21**, 299–307.

Dullien, F. A. L., 1979, *Porous Media, Fluid Transport and Pore Structure*, Academic Press, N.Y.

Fatt, I., 1956, The network model of porous media, I, II, III, *Trans. AIME*, **207**, 144–159, 160–163, 164–181.

Hassanizadeh, M. and Gray, W.G., 1979, General conservative equation for multi-phase systems: 1. Averaging technique, *Adv. Water Res.* **12**, (2), 131.

Johnson, N. L., 1949a, Systems of frequency curves generated by the method of translation, *Biometrika* **36**, 149–176.

Johnson, N. L., 1949b, Bivariate distributions based on simple translated systems, *Biometrika* **36**, 297.

Mustafa, N. A. and Marslia, M. L., 1983, Unsteady seepage analysis of Wallance dam, *Proc. ASCE*, **109**, 809–826.

Partom, I., 1978, Hydrodynamic dispersion in unsaturated flow through a porous medium, DSc Thesis (in Hebrew), Technion – Israel Institute of Technology, Haifa.

Shante, V. K. S. and Kirkpatrick, S., 1971, *Adv. Phys.* **42**, 395.